The SPARC Intercomparison of Middle Atmosphere Climatologies

W.J. Randel, E. Fleming, M.A. Geller, M.E. Gelman, K.P. Hamilton, D.J. Karoly, D.A. Ortland, S. Pawson, R. Swinbank, P.M. Udelhofen, F. Wu, M.P. Baldwin, M.-L. Chanin, P. Keckhut, K. Labitzke, E.E. Remsberg, A.J. Simmons, D. Wu

Our ability to evaluate general circulation models and new observations is limited by the availability and quality of datasets which describe the mean, or climatological, structure of the atmosphere. This paper presents a variety of climatological datasets of the middle atmosphere, which were produced using different techniques. Direct measurements include winds from rockets and radiosondes, and temperature from radiosondes. Space based radiance measurements can be inverted to give information about the thermal structure. Data assimilation systems, as well as other analysis techniques, combine data to give global or hemispheric maps. Various climatologies, produced either directly from the observations or using analysis techniqes are compared in this paper. The intention is to establish the confidence with which we understand the mean structure of the atmosphere and the limitations of various datasets. The mean state of the extratropics is quite well understood, with maximum differences of several degrees in the stratopause temperatures inferred using different datasets. In the Tropics there is a strong sensitivity, with large differences between the various observations and analyses. Direct wind observations give the strongest constraints on tropical winds, while temperatures (which can have large vertical gradients) are sensitive to the type of observations: sondes and limb-sounders are able to detect vertical structure which is obscured in nadir-sounding infrared radiance data. The results of this paper will be used for evaluating comprehensive climate models.

The SPARC Intercomparison of Middle Atmosphere Climatologies

William Randel[1]

Eric Fleming[2]

Marvin Geller[3]

Mel Gelman[4]

Kevin Hamilton[5]

David Karoly[6]

Dave Ortland[7]

Steve Pawson[2]

Richard Swinbank[8]

Petra Udelhofen*[3]

Fei Wu[1]

Mark Baldwin[7]

Marie-Lise Chanin[9]

Philippe Keckhut[9]

Karin Labitzke[12]

Ellis Remsberg[13]

Adrian Simmons[10]

Dong Wu[11]

[1]National Center for Atmospheric Research, Boulder, CO, USA
[2]NASA Goddard Space Flight Center, Greenbelt, MD, USA
[3]State University of New York at Stony Brook, Stony Brook, NY, USA
*deceased previously at StonyBrook
[4]National Centers for Environmental Prediction, Washington, DC, USA
[5]International Pacific Research Center, Honolulu, HI, USA
[6]Monach University, Melbourne, Australia
[7]Northwest Research Associates, Bellevue, WA, USA
[8]Met Office, Bracknell, United Kingdom
[9]Service d'Aeronomie, Paris, France
[10]European Center for Medium Range Weather Forecasts, Reading, United Kingdom
[11]Jet Propulsion Laboratory, Pasadena, CA, USA
[12]Free University of Berlin, Berlin, Germany
[13]NASA Langley Research Center, Hampton, VA

DRAFT (1/17) – January 2003

Abstract

Our current confidence in "observed" climatological winds and temperatures in the middle atmosphere (over altitudes ~10-80 km) is assessed by detailed intercomparisons of contemporary and historic data sets. These data sets include global meteorological analyses and assimilations, climatologies derived from research satellite measurements, and historical reference atmosphere circulation statistics. We also include comparisons with historical rocketsonde wind and temperature data, and with more recent lidar temperature measurements. The comparisons focus on a few basic circulation statistics, such as temperature, zonal wind, and eddy flux statistics. Special attention is focused on tropical winds and temperatures, where large differences exist among separate analyses. Assimilated data sets provide the most realistic tropical variability, but substantial differences exist among current schemes.

1. Introduction

Climatological data sets for the middle atmosphere are useful for empirical studies of climate and variability, and also necessary for constraining the behavior of numerical models. Current general circulation model (GCM) simulations routinely extend into the middle atmosphere (model tops at 50 km or higher), and require observational data sets for validation (e.g., Pawson et al., 2000). A number of middle atmosphere climatologies have been developed in the research community over the years, based on a variety of data sources and analysis techniques, and there are differences among these climatologies due to a number of reasons. For instance, the data sets are based on different combinations of radiosonde wind and temperature measurements and satellite temperature data, and global analyses are based a variety of objective statistical analyses and data assimilation techniques. Also, the fact that strong decadal-scale trends are observed in the stratosphere (Ramaswamy et al., 2001) means that a stratospheric climatology is itself time varying.

The earliest comprehensive climatologies for the middle atmosphere were the 1964 and 1972 COSPAR reference atmospheres (CIRA), which were based largely on interpolation of single station balloon and rocket data. An updated version of CIRA in 1986 included early satellite observations of the stratosphere and mesosphere and has served as a community standard since that time. Around 1979, daily meteorological analyses with significant stratospheric coverage that included operational satellite temperature soundings began, and more recently (~1991) sophisticated model-based data assimilation schemes began to produce stratospheric analyses. These analyses (supplemented in the 1990's by extensive retrospective reanalyses) have served as the basis for some more recent middle atmosphere climatologies. Also, satellite observations from the Upper Atmosphere Research Satellite (UARS - launched in 1991 and continuing to

operate in 2003) have provided additional climatological data sets for the middle atmosphere. Details of the circulation statistics derived from these various data sets will depend on several factors, including details of data inclusion and analysis techniques, and the respective time periods covered.

The scientific questions regarding middle atmosphere climatological data sets have been studied by a Stratosphere Reference Climatology Group, under the auspices of the World Climate Research Program (WCRP) Stratospheric Processes and Their Role in Climate (SPARC) program. This group decided that instead of constructing another climatology, two valuable contributions would be to (1) bring together climatological data sets currently in use, and make them available to the broader research community, and (2) make detailed intercomparisons of these data sets to highlight biases and uncertainties. The SPARC Data Center (http://www.sparc.sunysb.edu) was established partially in response to (1), and an extensive Technical Report of intercomparisons was compiled in response to (2) (SPARC, 2002). This paper includes a summary of the intercomparisons in that report, with further emphasis on assessing current uncertainties.

The analyses here bring together several middle atmosphere climatological data sets that are in current use in the research community, and make direct comparisons of some basic measured and derived quantities. The climatologies include those derived from global meteorological analyses and satellite data, plus results from two independent data sets: historical rocketsonde wind and temperature measurements (covering 1970-1989), plus lidar temperature data (covering the 1990's). The comparisons are used to identify biases in particular data sets, and also to highlight regions where there is relatively large uncertainty for particular quantifies (i.e., where large differences are found among several data sets). Where possible, we provide some brief explanations as to why there are

uncertainties and/or why the data sets might differ. However, more in-depth and detailed explanations are beyond the scope of this paper.

An important aspect of numerical modeling for the middle atmosphere is to simulate not just the time mean structure, but also temporal (interannual) variability (e.g., Pawson et al., 2000). The SPARC (2002) report includes comparisons of interannual variance statistics, but for brevity this paper highlights time mean quantities. Our comparisons focus particular attention on the tropics, where there are relatively large differences among middle atmosphere climatological wind and temperature data sets (in particular, for variability related to the semi-annual oscillation (SAO) and quasi-biennial oscillation (QBO)). We furthermore present some comparisons between the few available sources of mesospheric winds and temperatures.

All of the monthly mean data presented and compared here are available to the research community via the SPARC Data Center (http://www.sparc.sunysb.edu). This paper and the more extensive SPARC (2002) report are intended to be companions to those on-line data.

2. Climatological Data Sets for the Middle Atmosphere

A. Description of fundamental data and types of global analyses

Two fundamental types of observations contribute to global (or hemispheric) stratospheric analyses. Radiosondes provide vertical profiles of temperature, pressure and horizontal winds, covering the lowest 20-30 km of the atmosphere. The current radiosonde network provides approximately ~1100-1200 soundings per day, almost evenly split for measurements at 00UTC and 12UTC; the vast majority of stations are located over land masses of the Northern Hemisphere. Almost all of these soundings (> 1000) reach at least 100 hPa, with ~800 reaching 30 hPa, and ~350 reaching up to 10 hPa. Satellite-derived temperature profiles are the other major source of stratospheric data. Operational meteorological polar orbiting satellites provide near-global temperature profile retrievals twice daily up to ~50 km altitude, but have the drawback of relatively low vertical resolution (> 10 km) in the stratosphere. A series of operational NOAA satellites has been in orbit since late 1978, containing a suite of instruments that are collectively called the TIROS Operational Vertical Sounder (TOVS) (Smith et al., 1979). An improved set of temperature and humidity sounders (called the Advanced TOVS, or ATOVS) is now replacing the older TOVS series, beginning with the NOAA-15 satellite launched in May 1998. Temperature retrievals or radiances from TOVS and ATOVS data are a primary input to many of the global analyses here (including CPC, UKMO, UKTOVS, NCEP, ERA15 and ERA40 data sets; acronyms are described in Table 1).

Details of the various stratospheric analyses are described below, but the types of global or hemispheric analyses can be summarized as follows. The simplest analyses provide global or hemispheric fields based on hand-drawn analyses (FUB) or objective

analysis gridding techniques (CPC and UKTOVS). More sophisticated analyses can be derived by the use of numerical forecast models to predict first-guess fields, and incorporate observations by optimal data assimilation (UKMO, NCEP, ERA15 and ERA40 data). Most of the analyses discussed below are based on very similar radiosonde and satellite data, and so the differences revealed in our comparisons highlight the sensitivity of the final statistics to details of the data usage and analysis techniques.

B. Description of data sets

This section presents short descriptions of the climatological data sets included in the comparisons. These are intended to be brief, and more details for each analysis can be found in the listed references. Table 1 provides a summary list of some relevant details for each analysis. For brevity, each data set is referred to throughout this work by the following short acronyms.

1. UKMO (Met Office Stratospheric Analyses)

Since October 1991 stratospheric analyses have been produced daily using a stratosphere-troposphere version of the Met Office's data assimilation system (Swinbank and O'Neill, 1994). These analyses were formerly referred to as UK Meteorological Office (UKMO) stratospheric analyses, and that acronym is used here. The analyses consist of temperatures, wind components and geopotential heights on a global grid of resolution 2.5° latitude by 3.75° longitude, output on the UARS standard pressure levels (with six equally spaced levels per decade of pressure). The analyses span the range 1000-0.3 hPa (approximately 0-55 km).

The stratospheric analyses were originally produced as correlative data for the NASA UARS project, starting from October 1991. Since October 1995 the separate UARS assimilation system was discontinued, but stratospheric analyses continue to be

produced using a similar data assimilation system, which is run as part of the Met Office operational forecasting suite. Since November 2000 the Met Office stratospheric analyses have been produced using a new 3-D variational (3DVAR) data assimilation system (Lorenc et al., 2000).

2. UKTOVS (Met Office Analyses of TOVS Data)

The Met Office also produced regular stratospheric analyses (not part of a model assimilation) from measurements made by NOAA operational satellites. These analyses have been referred to in the research community as UKTOVS (which we retain here). Monthly means from these analyses are available for the period January 1979-April 1997. The analysis method is described by Bailey et al. (1993), and Scaife et al. (2000) present climatological data and interannual variations diagnosed from the UKTOVS data.

The UKTOVS fields are derived from an independent analysis of TOVS radiance measurements. The daily TOVS data were used to derive geopotential thickness values, covering the layers 100-20, 100-10, 100-5, 100-2 and 100-1 hPa. The thicknesses were then mapped onto a 5 degree resolution global grid, and added to the operational analysis of 100 hPa height (obtained from Met Office operational global analyses) to produce height fields up to 1 hPa. In turn, temperatures and horizontal balanced winds are derived from the height fields. Winds at the equator are interpolated from low latitudes, and resultant tropical variations (e.g., the QBO) are rather weak (as shown below).

3. CPC (Climate Prediction Center)

Operational daily analyses of stratospheric geopotential height and temperature fields have been produced by the Climate Prediction Center (CPC) of the US National Centers for Environmental Prediction (NCEP) since October 1978 (Gelman et al., 1986). These data

are referred to as CPC analyses (to differentiate from NCEP reanalyses). The CPC stratospheric analyses of temperature and geopotential height are based on a successive-correction objective analysis (Finger et al., 1965) for pressure levels 70, 50, 30, 10, 5, 2, 1 and 0.4 hPa, incorporating TOVS and ATOVS satellite data and radiosonde measurements (in the lower stratosphere of the NH). This analysis system has been nearly constant over time (October 1978-April 2001). Horizontal winds are derived from the geopotential data using the 'linear balance' technique (Randel, 1987). As a note, the CPC analyses were changed beginning in May 2001, with the data up to 10 hPa based on the NCEP operational analyses, and fields above 10 hPa based solely on ATOVS. Extensive climatologies of the stratosphere have been derived from these CPC data by Hamilton (1982), Geller et al. (1983) and Randel (1992).

The TOVS temperatures used in the CPC analyses have been provided by a series of operational NOAA satellites; these instruments do not yield identical radiance measurements for a variety of reasons, and derived temperatures may change substantially when a new instrument is introduced (Nash and Forrester, 1986). Finger et al. (1993) have compared the CPC temperatures in the upper stratosphere (pressure levels 5, 2, 1 and 0.4 hPa) with co-located rocketsonde and lidar data, and find systematic biases of order ± 3-6 K. Finger et al. (1993) provide a set of recommended corrections (dependent on time period and pressure level) to the CPC temperature analyses, which have been incorporated in the results here. However, in spite of these adjustments, the CPC analyses still probably retain artifacts of these satellite changes.

4. NCEP Reanalyses

The NCEP/National Center for Atmospheric Research (NCAR) reanalysis project uses a global numerical weather analysis/forecast system to perform data assimilation using

historical observations, spanning the time period from 1957 to the present (Kalnay et al., 1996). For brevity, the NCEP/NCAR reanalyses are referred to as NCEP here. The model used in the NCEP reanalysis has 28 vertical levels extending from the surface to ~40 km, and analyses of winds, temperatures and geopotential height are output on stratospheric pressure levels of 100, 70, 50, 30, 20 and 10 hPa.

5. ERA15 (ECMWF 15-year Reanalysis)

The European Center for Medium Range Weather Forecasts (ECMWF) produced a global reanalysis for the period 1979-1993, based on data assimilation coupled with a numerical forecast model (Gibson et al., 1997). The forecast model used in that work spanned pressure levels 1000-10 hPa, with analyses output on stratospheric pressure levels of 100, 50, 30 and 10 hPa. An important detail is that the 10 hPa analysis level is at the top level of the model, and this has a detrimental impact on results at this level (as shown in the comparisons below).

6. ERA40 (ECMWF 40-year Reanalysis)

ECMWF is also producing an updated reanalysis, termed ERA40, covering the period 1957-2001. ERA40 will be a comprehensive set of global meteorological analyses, including the stratosphere up to 1 hPa, based on the use of variational data assimilation techniques. One important difference from the ERA15 reanalyses (in addition to the increased vertical domain) is that ERA40 will directly assimilate TOVS and ATOVS radiances, as opposed to retrieved temperature profiles. While production of the full ERA40 reanalyses is an ongoing activity at present, we include here a subset of early production results for the time period 1992-1997. The ERA40 analyses are available on 23 standard pressure levels spanning 1000-1 hPa, and also on each of the 60 levels of the assimilation model.

7. FUB (Free University of Berlin Analyses)

The meteorological analyses from the Free University of Berlin (FUB) are northern hemispheric, gridded products at four levels: 100, 50, 30, and 10 hPa. Monthly mean data at these levels are available since 1957 (geopotential height) and 1964 (temperature) on a 10-degree grid, with an increase in resolution to five degrees in the early 1970s. Daily analyses are produced only at the three upper levels (i.e., not at 100 hPa) and are provided only every second day in northern summer, when the flow evolves slowly. The analyses are performed by hand (subjective analysis) by experienced personnel using station observations of geopotential height, wind, and temperature. Hydrostatic balance and the thermal wind are used as the analyses are built up from the 100-hPa tie-on level, for which data from FUB were used in the early years, but later operational products from the German Weather Service were substituted. These data are a valuable record of the NH stratosphere between 1957 and 2001, analyzed in a consistent and uniform manner throughout this period. Full details of the FUB analysis, together with the entire data set, are available in compact disk (CD) format (Labitzke et al., 2002).

8. CIRA86 Climatology

The COSPAR International Reference Atmosphere, 1986 (CIRA86) of zonal mean temperature, geopotential height, and zonal wind has been described in detail in Barnett and Corney (1985a, 1985b) and Fleming et al. (1988, 1990). These reference climatologies extend from 0-120 km and are based on a variety of data sources, briefly summarized here.

Temperatures for 1000-50 hPa are taken from the climatology of Oort (1983) which is based primarily on radiosonde data from the 1960s and early 1970s. Temperatures at 30

hPa over the NH are taken from analyses of the Free University of Berlin (FUB), and for the SH are taken from the radiosonde climatology of Knittel (1974). For 10-2.5 hPa, values are based on satellite data from the Nimbus 5 Selective Chopper Radiometer (SCR) averaged over 1973-1974. From 2.5-0.34 hPa (~40-56 km), the SCR data were merged with temperatures from the Nimbus 6 Pressure Modulator Radiometer (PMR) averaged over the period July 1975-June 1978. The PMR data were used exclusively for 0.34 hPa-0.01 hPa (~56-80 km). All values were merged to obtain a smooth transition between the original data sets.

The zonal wind climatology in the troposphere is taken from Oort (1983), with winds in the middle atmosphere above 100 hPa based on gradient winds derived from the geopotential height climatology. At the equator the zonal wind (above 100 hPa) is based on the second derivative of geopotential height (Fleming and Chandra, 1989). The winds between the equator and 15 S (15 N) are computed by linear interpolation.

9. HALOE Temperatures

The Halogen Occultation Experiment (HALOE) instrument on UARS provides analyses of temperatures in the altitude range ~45-85 km (Russell et al., 1993; Hervig et al., 1996; Remsberg et al., 2002). HALOE uses a solar occultation measurement technique, providing 15 sunrise and 15 sunset measurements per day, with each daily sunrise or sunset group near the same latitude on a given day. The latitudinal sampling progresses in time, so that much of the latitude range ~ 60°N-S is sampled in one month; the measurements extend to polar regions during spring through late summer. The vertical resolution of these data are ~2 km, with sampling on UARS standard pressure levels (6 levels per decade of pressure). The results included here are based on HALOE retrieval version 19.

The seasonal temperature analyses here use the combined sunrise plus sunset temperatures binned into monthly samples. The seasonal cycle is derived by a harmonic regression analysis of these monthly data over the period January 1992-December 1999, including annual and semi-annual harmonics at each height and latitude (spanning 60°N-S). This regression provides a useful method of interpolating the irregular temporal sampling of HALOE.

10. MLS Temperatures

Middle atmosphere temperatures have also been obtained from the Microwave Limb Sounder (MLS) instrument on UARS (Fishbein et al., 1996). The data here are from an independent retrieval described in Wu et al. (2002), covering the time period January 1992-December 1994. This retrieval is completely independent of other climatologies, using a single temperature profile (an annual mean) as the first guess and linearization point. The valid altitude range is 20-90 km, with large uncertainties at the two ends; the temperature is reported on the UARS standard pressure grid (six per decade of pressure), but the actual retrieval was carried out at every other pressure surface. Compared to the MLS Version 5 (V5) retrieval, the data here have much better vertical resolution in the mesosphere, while it is about the same in the stratosphere. These data and further descriptions are available to the research community via an ftp site: mls.jpl.nasa.gov/pub/outgoing/dwu/temp.

The orbital characteristics of UARS allow MLS to obtain data from approximately 80°S-32°N or 32°S-80°N for alternating satellite yaw cycles (each approximately one month long). In order to handle these large data gaps in high latitudes, our analyses fit the seasonal cycle at each latitude and pressure level using harmonic regression analyses of monthly sampled data (including annual and semiannual harmonic terms in the analyses).

11. URAP Reference Atmosphere Winds

As part of the UARS Reference Atmosphere Project (URAP), Swinbank and Ortland (2002) compiled a wind data set using measurements from the UARS High Resolution Doppler Imager (HRDI; Hays et al., 1993), supplemented with data from the Met Office stratospheric analyses (UKMO). The data set comprises zonal-mean wind data from the earth's surface to the lower thermosphere every month for a period of about 8 years starting from the launch of UARS, and the climatology here use statistics averaged over 1992-1998. The wind data are archived on the UARS standard pressure levels, for latitudes from 80°S to 80°N.

Mesospheric wind measurements from HRDI extend from the middle mesosphere (above ~60 km) to the lower thermosphere. These HRDI measurements were combined with UKMO stratospheric analyses (up to ~56 km) to provide near continuous coverage in altitude (with balance winds derived for the gap region); see Swinbank and Ortland (2002) for details. Figure 1 shows January and July climatological zonal winds derived from the URAP data set, highlighting the continuous data availability over 0-85 km (note the deep vertical structure of the stratospheric-mesospheric jet structures). For reference, Figure 1 also includes corresponding temperature climatologies, derived from combined UKMO, HALOE and MLS data (as described in SPARC, 2002).

Table 1. Middle Atmosphere Data Sets Included in the SPARC Intercomparisons

Data Source	Acronym	Reference	Type of Analysis	Time Period Available
Met Office Stratospheric Analyses	UKMO	Swinbank and O'Neill, 1994	Assimilation	Nov. 1991-present
Met Office TOVS Analyses	UKTOVS	Bailey et al., 1993	Objective analysis	Jan. 1979-Apr 1997
NCEP Climate Prediction Center	CPC	Gelman et al., 1986	Objective analysis (above 100 hPa)	Oct. 1978-present
NCEP reanalysis	NCEP	Kalnay et al., 1996	Assimilation	1957-present
ERA15 reanalysis	ERA15	Gibson et al., 1997	Assimilation	1979-1993
ERA40 reanalysis	ERA40		Assimilation	1957-2001
Berlin Stratospheric Analyses	FUB	Labitzke et al., 2002	Historical analysis (NH only)	1957-2001
CIRA86 climatology	CIRA86	Fleming et al., 1990	Various	Various (1960's-1970's)
HALOE temperatures	HALOE	Russell et al., 1993	Harmonic analysis of seasonal cycle	1992-2001
MLS temperatures	MLS	Wu et al., 2002	Harmonic analysis of seasonal cycle	Jan. 1992-Dec. 1994
UARS Reference Atmosphere Program zonal winds	URAP	Swinbank and Ortland, 2002	UKMO and HRDI data	Jan. 1992-Dec. 1998

C. Rocketsonde wind and temperature data

Measurements from small meteorological rockets provide an important source of in situ wind and temperature information for the middle atmosphere, in the 25 to 85 km altitude region. A program of rocketsonde measurements began in the United States in the late 1950s, and expanded during the 1960's to about a dozen stations making regular measurements once to three times per week. The number of rocketsonde measurements peaked in the late 1970s, at about 1000 to 1500 yearly, including measurements from the former Soviet Union (USSR), Japan and several other countries. Most measurement locations were at middle latitudes of the northern hemisphere and tropical locations. The number of rocketsonde stations and frequency of observations decreased markedly in the 1980s, and by the 1990s fewer than 100 rocketsonde measurements were made globally each year. Details of the rocketsonde measurement technique and their uncertainty characteristics are discussed in SPARC (2002).

The rocketsonde wind and temperature climatologies shown here are based on simple monthly averages, derived by binning all of the available observations during 1970-1989. Figure 2a shows the availability of rocketsonde observations for this period as a function of latitude. Due to data availability, we focus the comparisons on the tropics and extratropical NH. The extratropical bins are centered at 30°, 60°, and 80° latitude, including measurements within ± 10° of the central latitude. The tropical data are separated for measurements near 10°S (mostly from Ascension Is. at 8°S), and near 10°N (mostly from Kwajelein at 8°N and Ft. Sherman at 9°N). Based on this sampling, there are approximately 100-300 profile observations in each monthly bin, depending on latitude and altitude. Vertical sampling is made on the UARS pressure grid (six levels per decade of pressure).

Two important considerations apply to the comparisons of rocketsonde data with global analyses. First, the time periods compared here for the data are different (1992-1997 for the analyses, and 1970-1989 for the rocketsondes). This is most important for temperatures in the upper stratosphere and mesosphere, which have experienced strong cooling (of order 2 K/decade near the stratopause, and possibly larger in the mesosphere) during the recent decades (Dunkerton et al., 1998; Ramaswamy et al., 2001). A large part of the observed rocketsonde-analyses differences in these regions can be attributed to this cooling. Second, the monthly samples from analyses are based on zonal and monthly means of daily data, whereas the rocketsonde statistics are derived from infrequent samples at specific locations, taken over many years. Thus variability levels for the rocketsonde means are significantly larger. Estimates of the standard error for the monthly rocketsonde (and lidar) data are calculated as $\sigma_{climatology} = \sigma/\sqrt{N}$, where σ is the standard deviation of the individual soundings within each month and latitude bin, and N is the number of measurements.

D. Lidar temperature data

Lidars provide measurements of the vertical temperature profile in the middle atmosphere, and a number of specific sites have made lidar temperature measurements for a decade or longer. The Rayleigh lidar technique uses the backscattering of a pulsed laser beam to derive the vertical profile of atmospheric density, from which the temperature profile is deduced (Hauchecorne and Chanin, 1980; Keckhut et al., 1993). This technique provides an absolute temperature measurement over altitudes ~30-75 km, which does not require adjustment or external calibration. The vertical resolution of the lidar data is approximately 3 km, and the profiles here are sampled on the UARS standard pressure grid.

For the climatological analyses here, we obtained a number of lidar temperature time series (for stations with relatively long records) from the Network for the Detection of Stratospheric Change (NDSC) web site: http://www.ndsc.ws/. The specific locations and available time records are listed in Table 2. The individual profiles are binned into monthly samples, focused on latitude bins centered at 20°N, 40°N and 80°N. We use all the lidar observations over 1990-1999, in order to most directly compare with the meteorological analyses over 1992-1997 (a slightly longer time record for the lidar data provides better monthly sampling). The total number of lidar observations and their latitudinal sampling is shown in Figure 2b. Our monthly and latitudinal sampling produces between ~20-80 measurements per bin for latitudes 20°N, and 80°N, and ~300 per month for the bin centered at 40°N. The associated monthly means and standard deviations are calculated identically to those for the rocketsonde analyses.

Table 2.
Lidar temperature data obtained from the NDSC web site: http://www.ndsc.ws/

Location	available time period
Eureka (80°N)	1993-1998
Ny Alesund (79°N)	1995-1998
Thule (77°N)	1993-1995
Hohenpeissenberg (48°N)	1987-1999
OHP (45°N)	1991-2000
Toronto (44°N)	1996-1997
Table Mountain (34°N)	1989-2001
Mauna Loa (20°N)	1993-2001
Reunion (22°S)	1994-1998

3. Data Intercomparisons

In this section direct comparisons are made among the different data sets for monthly mean global fields of temperature and zonal winds. The first requirement for such comparisons is to choose a time period which maximizes record length for overlap among

most data sets. Here we choose the period January 1992-December 1997, which gives direct overlap of the UKMO, CPC, NCEP and ERA40 reanalysis, and FUB fields. The UKTOVS record is slightly shorter (to April 1997). The ERA15 reanalysis has a much shorter record during this 1992-1997 period (January 1992-December 1993). We include comparisons for these data by calculating *differences* only over this 1992-1993 record, rather than the full 6 years 1992-1997. We also include comparisons with the CIRA86 climatology, although it should be kept in mind that these data are derived from a very different time period (covering the 1960's-1970's). Rocketsonde data span 1970-1989, while lidar temperatures cover 1990-1999.

A. Temperature

1. Zonal mean climatology

The latitudinal structure of 100 hPa temperature in January for each analysis is shown in Figure 3a. The overall latitudinal structure is similar in each data set, and comparisons are best made by considering differences with a single standard (UKMO in this case; note this is not an endorsement of the UKMO analyses as 'better' or more 'correct', but simply a choice of using one data set as a reference). Differences with the UKMO 100 hPa analyses are shown in Figure 3b, showing largest differences in the tropics and also over the Arctic. These tropical and polar differences are also observed in other months (not shown here), and discussed in turn below. Aside from UKTOVS data (which are an outlier, and not included in Figure 3b), the 100 hPa tropical temperatures fall into two groups, biased warmer (CPC, NCEP and CIRA86) or colder (FUB,ERA15 and ERA40) than UKMO. As discussed in more detail below, the latter (cold) group is

probably more realistic, and the former data sets (plus UKMO) have a true warm tropical bias of ~2-3 K at 100 hPa.

As seen in Figure 3, there can be substantial differences in climatologies of polar temperature in the lower stratosphere. Figure 4 compares the seasonal cycle of 50 hPa zonal mean temperature in both polar regions (80 N and 80 S), including their respective differences from UKMO analyses. The CIRA86 data exhibit warm biases by up to ~5 K in the Arctic and ~10 K in the Antarctic, maximizing during winter-spring in each hemisphere. A large portion of these differences reflects true cooling in the polar lower stratosphere between the 1960's and 1990's (e.g., Randel and Wu, 1999; Ramaswamy, 2001). Aside from CIRA86, the other climatologies agree to approximately ± 1 K in the Arctic and ± 2 K in the Antarctic. Most analyses are colder than UKMO during Arctic winter, suggesting a small warm UKMO bias. Manney et al. (1996) compared CPC and UKMO data with polar radiosondes during several winters, finding systematic warm biases (of order 1-3 K) for both CPC and UKMO data in the Arctic. In the Antarctic the CPC data showed similar 1-2 K warm biases, while UKMO biases were smaller (< 1 K). These comparisons are consistent with the results in Figure 4.

Zonal mean temperature comparisons in the middle and upper stratosphere show relatively larger differences (typically ± 2-4 K) than at 100 or 50 hPa, and each data set has characteristic patterns of differences (typically larger over high latitudes). The CIRA86 and MLS data are consistently on the warm side of the ensemble throughout the stratosphere, while ERA40 has cold biases over ~5-2 hPa. NCEP and ERA15 data have persistent biases near 10 hPa, which is the top level of their analyses. Comparisons at 1 hPa (see below) show a range of mean differences of order ~5 K. This level near the stratopause presents special problems in analyses, because it is not captured accurately in

TOVS thick layer radiance measurements, plus it is near the top of the UKMO forecast/assimilation model (at 0.3 hPa).

a. Comparisons with rocketsondes

As shown in Figure 2a, most of the extratropical rocketsonde data occur in latitude bins near 30°N, 60°N and 80°N. Figure 5 compares rocketsonde climatological temperature profiles with analyses at 30°N for January. The rocketsondes show good overall agreement in the stratosphere, and in locating the altitude of the stratopause. The rocketsonde temperatures in the mesosphere (~50-70 km) are warmer than the HALOE and MLS climatologies, and this is a consistent feature of the rocketsondes that is at least partially due to the differing respective time periods.

The seasonal variation of temperatures near 30°N from rocketsondes and analyses are compared in Figure 6, for data at 1 and 0.1 hPa. At 1 hPa there are mean biases of order 5 K between the climatologies, and the rocketsonde temperatures are on the warm side of the ensemble. At 0.1 hPa the mean rocketsonde values are ~4-10 K warmer than MLS or HALOE data, and ~2-8 K warmer than CIRA86, and the rocketsonde differences are largest during NH winter (October-March). Even larger rocketsonde differences (~10-20 K) are found for comparisons at 60°N (SPARC, 2002).

b. Comparisons with lidars

The lidar temperature measurements are contemporaneous with the global analyses, and offer the most direct comparisons. Lidars have the most data available in the latitude bands near 20°N and 40°N (Figure 2b), and we focus here on comparisons near 40°N (lidar measurements from Table Mountain, OHP, Hohenpeissenberg and Toronto). The seasonal comparison of temperatures at 10, 1 and 0.1 hPa are shown in Figure 7. The comparisons

at 10 hPa show excellent agreement (with CIRA86 and UKTOVS as warm outliers). The lidars fall in the mid-range of analyses at 1 hPa, and exhibit reasonably good agreement at 0.1 hPa (although biased warm during equinox seasons). We note that the overall good agreement between the lidars and satellite data at 0.1 hPa in Figure 7 is further evidence that the larger differences with rocketsondes in the mesosphere (Figures 5-6) are primarily due to the different time periods covered.

Lidar data for the Arctic region are primarily available during winter, and a seasonal comparison is not possible. Figure 8 shows profile comparisons for 80°N for DJF, based on lidar data from Eureka, Ny Alesund and Thule. The lidars and most analyses show reasonable agreement up to the stratopause (differences of ~ ± 2-3 K). The ERA40 reanalysis exhibits cold biases of order 5 K in the upper stratosphere (~5-2 hPa), and this is a persistent bias observed at all latitudes. The cause of this problem is under review at ECMWF. The lidar data are ~5-10 K colder than the MLS and CIRA86 data in the polar mesosphere.

2. Tropical seasonal cycle in temperature

The tropics present special problems for analysis of stratospheric temperatures and winds. The tropical tropopause temperature minimum has a sharp vertical structure that is not well resolved by satellite measurements, and it is also problematic for assimilation/forecast models with vertical resolution of ~2 km. Temperature anomalies associated with the quasibiennial oscillation (QBO) have relatively shallow vertical structures, which are also poorly resolved by nadir-viewing operational satellites. Thus it is not surprising to find a wide variance between climatological data sets in the tropics. Here we focus on the seasonal variability in each data set; these analyses complement the tropical data comparisons shown in Pawson and Fiorino (1998a, b).

The seasonal variations of equatorial temperature at 100 and 50 hPa derived from each climatological data set are shown in Figure 9. Included in these figures are estimates of monthly temperatures derived for the same 1992-1997 time period from radiosonde measurements at a group of eight near-equatorial stations (within 5° of the equator, including Belem, Bogota, Cayenne, Manaus, Nairobi, Seychelles, Singapore and Tarawa). The amplitude of the seasonal cycle in temperature is reasonably well captured in most data sets at 100 hPa, but there are clear biases among the data sets. In particular, the ERA15, ERA40 and FUB data are the coldest and agree best with radiosondes (except for FUB during January-March), whereas UKMO, CPC, NCEP and CIRA86 data each have a consistent warm bias of ~2-3 K (and UKTOVS is almost 10 K too warm, and not shown in Figure 9). At 50 hPa the CPC, NCEP and ERA40 data agree best with radiosondes, with FUB ~2 K warmer during NH winter-spring. The UKMO analyses appear warm at 50 hPa, but the comparison is not exact since the UKMO pressure level is 46.4 hPa. The CIRA86 and UKTOVS (not shown) are warm outliers at 50 hPa.

a. Semi-annual oscillation (SAO)

Seasonal temperature variations in the tropics at and above 10 hPa are dominated by a semi-annual oscillation (SAO), and here we quantify the SAO amplitude and phase structures derived from the different data sets. A comprehensive review and climatology of the SAO (extending to 100 km) is provided in Garcia et al. (1997). The results here are based on simple harmonic analyses of the different data sets for the time periods available.

Figure 10a shows the amplitude structure of the temperature SAO as a function of latitude at 2 hPa as derived from the different data sets. The temperature SAO has a

maximum over the equator, falling to small amplitudes at 20°N/S. The different data sets in Figure 10 show a clear separation in terms of SAO amplitude, with the ERA40, MLS, HALOE and CIRA86 data having amplitudes near 4 K, approximately twice as large as the CPC, UKMO and UKTOVS results. The rocketsonde results (shown as dots near 8°N and 8°S) show amplitudes that agree better with values from the former (larger amplitude) group. Note, however, that because the rocketsonde measurement are not directly over the equator, they do not capture the full magnitude of the SAO. Phases at 2 hPa (not shown) are in good agreement between all data sets (first maximum in the year near April 1).

The vertical structure of the temperature SAO amplitude and phase at the equator are shown in Figures 10b-c, including results from each data set. Rocketsonde results are included by averaging results at 8°N and 8°S (see Figure 10a), with amplitudes multiplied by a factor of 1.3 to approximate equivalent equatorial values. As well-known from previous analyses (e.g., Hirota, 1980), the temperature SAO has a double peaked structure in altitude, with maxima below the stratopause (~ 45 km) and mesopause (~ 70 km), and these maxima are approximately out of phase. As noted above, the maximum near 45 km has an amplitude of ~4 K in MLS, HALOE, CIRA86, ERA40 and rocketsonde data sets, and substantially weaker amplitude in CPC, UKMO and UKTOVS data. For the maximum near 70 km the CIRA86, MLS and HALOE show a range of amplitudes of ~4-7 K. For further comparison of the upper level peak, the open circles in Figure 10 show results derived from Solar Mesosphere Explorer (SME) temperature data for 1982-1986 (taken from Garcia and Clancy, 1990). These SME results show similar amplitude and phases as the other data sets, but don't exhibit an absolute peak near 70 km.

B. Zonal mean zonal winds

1. Zonal mean climatology

Climatological zonal mean zonal winds show overall good agreement among the various data sets in extratropics, whereas relatively large differences occur in the tropics. Tropical stratospheric winds present particular problems, because there are few direct wind measurements above the lower stratosphere. Also, due to the smallness of the Coriolis parameter, determination of balanced winds in the tropics require more accurate estimates of horizontal temperature gradients. Figure 11 shows cross sections of differences (from UKMO analyses) of January average zonal winds for CPC, ERA40 and CIRA86 data (i.e., differences from the January climatology shown in Figure 1). Differences in extratropics for CPC and ERA40 are of order ~2 m/s, and this is typical for other months (and for NCEP, ERA15 and UKTOVS data); slightly larger extratropical differences (up to ~10 m/s) are found for CIRA86 data. Relatively larger zonal wind differences are seen in the tropics in Figure 11, and this is typical across all the data sets. Strong tropical easterly biases are a particular problem in the CIRA86 data set.

Further comparisons of zonal winds in the upper stratosphere and mesosphere are shown in Figure 12, including results from rocketsondes (which provide direct measurements of zonal winds, and are unique for comparing to analyses). Figure 12 shows statistics at 10°S and 30°N, for 5 and 0.1 hPa. In the upper stratosphere the rocketsondes show good agreement with analyses both in the tropics and extratropics. Furthermore, the few available data sets in the mesosphere (CIRA86, URAP and rocketsondes) show reasonably similar seasonal variability; note that the strength of the subtropical mesospheric jet near 30°N (maximum over November-January; see Figure 1) is echoed in each data set.

a. Tropical semi-annual oscillation

As with temperature, the SAO dominates the seasonal variation of zonal winds in the tropics above the middle stratosphere. The latitudinal amplitude structure of the zonal wind SAO at 1 hPa is shown in Figure 13a, comparing each data set along with rocketsonde results at 8°N and 8°S. The zonal wind SAO shows maximum amplitude near 10-20°S for most data sets, which is distinct from the equatorially-centered SAO in temperature (Figure 10a). The rocketsonde results near 8°N and 8°S suggest a latitudinal asymmetry consistent with analyses i.e., larger zonal wind SAO in the SH subtropics. The rocketsonde SAO amplitudes are approximately 25% larger than most analyses (except for ERA40), while the phases (not shown) are in good agreement. Figures 13b-c show the SAO vertical amplitude and phase structure at the equator, including rocketsonde results (taken as averages of 8°N and 8°S). The vertical structure shows an amplitude maximum near the stratopause (~50 km), with a magnitude of ~15-20 m/s for the analyses; the rocketsondes give a maximum up to 25 m/s. A second amplitude maximum near the mesopause (~80 km) is suggested in URAP and CIRA86 winds.

b. The QBO

Figure 14 shows interannual anomalies in equatorial zonal wind at 30 and 10 hPa during 1988-1997 derived from the various analyses. The QBO dominates variability in these time series, and included in Figure 14 are anomalies derived from Singapore radiosonde data, which are a standard reference for the QBO (e.g., Naujokat, 1986). The QBO signal is evident in each analysis, but the amplitude varies strongly between different data (and with altitude). In general the assimilated data sets (UKMO, NCEP, ERA15 and ERA40) have the largest, most realistic amplitudes, whereas the balance winds derived from CPC and UKTOVS are much too weak. No analysis data set captures the strength of the 10 hPa easterlies observed at Singapore. The strength of the zonal wind QBO in the

different data sets is quantified in Figure 15, where the equivalent QBO amplitude (defined as $\sqrt{2}$•rms deviation of deseasonalized anomalies during 1992-1997) is plotted as a function of latitude (at 30 hPa) and height. For comparison, Figure 15 also includes the 30 hPa QBO amplitude derived from tropical radiosonde climatologies in Dunkerton and Delisi (1985), plus the equivalent result from Singapore radiosonde measurements over pressure levels 70-10 hPa. Furthermore, Figure 15 includes an equivalent QBO amplitude derived from rocketsonde data during 1970-1989, for altitudes ~24-37 km (where a strong QBO is evident by eye in the deseasonalized time series). For the analyses data sets the ERA40 exhibits the largest QBO amplitude (in best agreement with the radiosonde climatology and Singapore data), with the ERA15, UKMO and NCEP reanalyses somewhat weaker, and CPC and UKTOVS (balance winds) as severe underestimates. The ERA40, ERA15, UKMO and NCEP data sets show approximately similar amplitudes between 70 and 30 hPh, whereas above 30 hPa there are larger differences. Only the ERA40 approaches the Singapore and rocketsonde amplitudes over 20-10 hPa, although Figure 14 shows significant differences in detail (especially for the easterly phase). Above 10 hPa there is a factor of two difference between the ERA40 and UKMO results, and here the UKMO data are almost certainly too weak.

C. Zonal averaged heat and momentum fluxes

The zonally averaged fluxes of heat $\left(\overline{v'T'}\right)$ and momentum $\left(\overline{u'v'}\right)$ are fundamentally important diagnostics of atmospheric wave behavior and large-scale transport. Their calculation is based on covariances of eddy winds and temperatures (in longitude), and these fluxes provide sensitive diagnostics of planetary wave behavior and coupling with the

mean flow via the Eliassen-Palm (EP) flux and its divergence (Andrews et al., 1987). Of primary importance is the poleward eddy heat flux $\left(\overline{v'T'}\right)$ in the extratropical lower stratosphere, which is proportional to the vertical wave activity flux (EP flux) from the troposphere into the stratosphere. The fluxes considered here are calculated from daily data and then monthly averaged (i.e., they contain both stationary and transient components), compared for the period 1992-1997. Because daily data are involved in these calculations, the comparisons here are limited to UKMO, CPC, NCEP and ERA40 reanalyses (and note that the CPC results are based on balance wind calculations).

Poleward eddy heat fluxes in the lower stratosphere maximize over approximately 40-70° in each hemisphere, with similar latitudinal structures for each data set. The seasonal variations of $\overline{v'T'}$ averaged over 40-70°N and 40-70°S at 100 hPa from each data set are compared in Figure 16. The magnitude of $\left(\overline{v'T'}\right)$ in the NH varies by ~ 10-20% between the analyses, with ERA40 and NCEP on the stronger side and CPC slightly weaker. These uncertainties are consistent with Newman and Nash (2000), who include comparisons with other data sets (for shorter periods). This 10-20% difference is thus the current level of uncertainty in this derived quantity over NH midlatitudes. Similar statistics for the SH in Figure 16 show the CPC data as an outlier with substantially smaller fluxes than the other analyses; the ERA40 data show significantly stronger fluxes during the active months of September-December. Qualitatively similar results are found for comparisons of stratospheric momentum fluxes $\left(\overline{u'v'}\right)$ in SPARC (2002). Namely, NH statistics show differences of ~20%, and CPC data are an outlier with relatively small values in the SH.

4. Summary: Biases and outstanding uncertainties

This study has focused on comparing climatological data sets for the middle atmosphere which are currently used in the research community. Overall the climatologies developed from analyses (and lidar measurements) for the 1990's agree well in most aspects, although each global data set can exhibit 'outlier' behavior for certain statistics. The following is a list of the largest apparent biases in each climatological data set, as derived from the intercomparisons discussed here and in SPARC (2002). These are identified when individual data sets are 'outliers' from the group, for these particular features.

UKMO
- cold temperature biases (~5 K) near the stratopause (globally)
- warm tropical tropopause temperature (1-2 K)

UKTOVS
- large temperature biases (~ ± 3-5 K) in low latitudes (~ 30°N-S) over much of the stratosphere (20-50 km)
- winter polar night jets somewhat too strong
- weak tropical wind variability (derived from balanced winds)

CPC
- warm temperature biases (~1-3 K) in the Antarctic lower stratosphere during winter-spring
- weak tropical wind variability (derived from balanced winds)
- warm tropical tropopause temperatures (2-3 K)
- weak eddy fluxes in SH

NCEP
- warm tropical tropopause (2-3 K)

- satellite data discontinuity across 1978-1979

ERA15
- global cold biases (~3 K) at 30 and 10 hPa

ERA40
- cold temperature biases (~5 K) in the upper stratosphere
- oscillatory vertical structure in temperature, especially large over Antartica

CIRA86
- warm biases of ~5-10 K over much of the stratosphere (20-50 km)
- relatively large easterly biases in tropical winds (derived from balanced winds)
- SAO's in mesospheric wind and temperature not well resolved

MLS
- warm biases (~3-7 K) over much of the stratosphere (20-50 km)

Comparisons of the recent climatologies with the historical data sets (CIRA86 and rocketsondes) show reasonable agreement, but the effect of decadal-scale cooling throughout the middle atmosphere is evident, particularly in the polar lower stratosphere (Figure 4) and in the upper stratosphere and mesosphere (e.g., Figures 5-6). Decadal changes may also influence zonal mean winds at high latitudes (SPARC, 2002). Despite these differences, the overall quality of the CIRA86 global climatologies is remarkable, given that they were derived from several combined data sets, covering different altitudes and time periods. While the direct wind measurements afforded by UARS and data assimilation techniques provide improved winds (especially in the tropics), the balance wind calculations of CIRA86 captured the overall global climatology reasonably well.

The comparisons here also allow us to highlight aspects of middle atmosphere climatologies which are relatively uncertain. These are identified for statistics that show relatively large variability among each of the different data sets, suggesting a fundamental level of uncertainty or high sensitivity to the details of data analysis. These include:

1) The tropical tropopause region is biased warm (compared to radiosonde data) in many analyses. Relatively smaller biases are found in the ERA15, ERA40 and FUB analyses, which are more strongly tied to radiosonde measurements. The warm biases in this region of sharp temperature gradients probably result from a combination of low vertical resolution in the analyses, plus the less than optimal use by most analyses of thick-layer satellite temperature measurements.
2) The temperature and 'sharpness' of the global stratopause shows considerable variability among different data sets. This is probably due to the relatively low vertical resolution of TOVS satellite measurements, and also the fact that the stratopause is near the upper boundary for several analyses (UKMO, CPC, UKTOVS).
3) Temperature variability in the tropical upper stratosphere (associated with the SAO) is underestimated in analyses that rely primarily on low resolution TOVS satellite data (CPC, UKTOVS and UKMO).
4) QBO variations in temperature and zonal wind are underestimated to some degree in most analyses, as compared to Singapore radiosonde data. The best results are derived from assimilated data sets (ERA40, ERA15, UKMO and NCEP, in that order) and only ERA40 has realistic zonal wind amplitudes above 30 hPa. The use of balance winds in the tropics (derived from geopotential data alone) is problematic for the QBO, and produces large underestimates of variability in the CPC and UKTOVS data sets.

The overall improvements seen in the ERA40 data for tropical variability suggests that improving data assimilation techniques offer the best opportunity for accurate analyses in the tropical stratosphere.

Acknowledgments

These climatological comparisons have resulted from work of the SPARC Reference Climatology Group, which has been ongoing since 1994. A majority of the work has centered around obtaining and archiving the numerous data sets in the SPARC Data Center. This activity was primarily organized by Dr. Petra Udelhofen, who unfortunately died during the final stages of preparation of the SPARC (2002) report. Petra was a valued friend and colleague of everyone involved with this project, and we dedicate it to her memory.

We wish to note special thanks to the NASA ACMAP Research Program, for support of the SPARC Data Center, and for supporting several individuals involved with the Climatology Group. Marilena Stone (NCAR) expertly prepared the manuscript through many drafts.

4. References

Andrews, D. G., J. R. Holton and C. B. Leovy, Middle Atmosphere Dynamics. Academic Press, 1987.

Bailey, M. J. A. O'Neill and V. D. Pope, Stratospheric analyses produced by the United Kingdom Meteorological Office, J. Appl. Meteorol., 32, 1472-1483, 1993.

Barnett, J. J. and M. Corney, Temperature data from satellites, "Middle Atmosphere Program, Handbook for MAP," Vol. 16, edited by K. Labitzke, J. J. Barnett and B. Edwards, 2-11, 1985a.

Barnett, J. J. and M. Corney, Middle atmosphere reference model from satellite data, "Middle Atmosphere Program, Handbook for MAP," Vol. 16, edited by K. Labitzke, J. J. Barnett and B. Edwards, 47-85, 1985b.

Dunkerton, T. J. and D. P. Delisi, Climatology of the equatorial lower stratosphere, J. Atmos. Sci., 42, 376-396, 1985.

Dunkerton, T., D. Delisi and M. Baldwin, Examination of middle atmosphere cooling trend in historical rocketsonde data, Geophys. Res. Lett., 25, 3371-3374, 1998.

Finger, F. G., H. M. Wolf and C. E. Anderson, A method for objective analysis of stratospheric constant pressure charts, Mon. Wea. Rev., 93, 619-638, 1965.

Finger, F. G., M. E. Gelman, J. D. Wild, M. L. Chanin, A. Hauchecorne and A. J. Miller, Evaluation of NMC upper stratospheric analyses using rocketsone and lidar data, Bull. Amer. Meteor. Soc., 74, 789-799, 1993.

Fishbein, E., et al., Validation of the UARS Microwave Limb Sounder temperature and pressure measurements, J. Geophys. Res., 101, 9983-10,016, 1996.

Fleming, E. L., S. Chandra, M. R. Schoeberl and J. J. Barnett, Monthly mean global climatology of temperature, wind, geopotential height, and pressure for 0-120 km, NASA Tech. Memo, NASA TM-100697, 85 pp., 1988.

Fleming, E. L. and S. Chandra, Equatorial zonal wind in the middle atmosphere derived from geopotential height and temperature data, J. Atmos. Sci., Vol. 46, 860-866, 1989.

Fleming, E. L., S. Chandra, J. J. Barnett and M. Corney, Zonal mean temperature, pressure, zonal wind, and geopotential height as functions of latitude, COSPAR International Reference Atmosphere: 1986, Part II: Middle Atmosphere Models, Adv. Space Res., 10, No. 12, 11-59, 1990.

Garcia, R. R. and R. T. Clancy, Seasonal variation of equatorial mesospheric temperatures observed by SME, J. Atmos. Sci., 47, 1666-1673, 1990.

Garcia, R. R., T. J. Dunkerton, R. S. Lieberman and R. A. Vincent, Climatology of the semiannual oscillation of the tropical middle atmosphere, J. Geophys. Res., 102, 26,019-26,032, 1997.

Geller, M. A., M.-F. Wu and M. E. Gelman, Troposphere-stratosphere (surface-55 km) monthly winter general circulation statistics for the Northern Hemisphere-Four year averages, J. Atmos. Sci., 40, 1334-1352, 1983.

Gelman, M. E., A. J. Miller, K. W. Jihnson and R. N. Nagatani, Detection of long term trends in global stratospheric temperature from NMC analyses derived from NOAA satellite data, Adv. Sp. Res., 6, 17-26, 1986.

Gibson, J. K., et al., ERA description, Reanalysis Project Rept. 1, Eur. Center for Medium-Range Weather Forecasts, Reading, England, 1997.

Gray, L. J., S. Phipps, T. Dunkerton, M. Baldwin, E. Drysdale and M. Allen, A data study of the influence of the equatorial upper stratosphere on Northern Hemisphere stratospheric sudden warmings, Q.J.R. Meteorol. Soc., 127, 1985-2004, 2001.

Hamilton, K., Stratospheric Circulation Statistics. NCAR Technical Note NCAR/TN-191 STR, 174 pp., 1982.

Hauchecorne, A. and M.-L. Chanin, Density and temperature profiles obtained by lidar between 35 and 70 km, Geophys. Res. Lett., 7, 565-568, 1980.

Hays, P. B., V. J. Arbreu, M. E. Dobbs, D. A. Gell, H. J. Grassl and W. R. Skinner, The high-resolution Doppler imager on the Upper Atmosphere Research Satellite, J. Geophys. Res., 98, 10,713-10,723, 1993.

Hervig, M. E., et al., Validation of temperature measurements from the Halogen Occultation Experiment, J. Geophys. Res., 101, 10,277-10,286, 1996.

Hirota, I., Observational evidence of the semiannual oscillation in the middle atmosphere: A review, Pine Appl. Geophys., 118, 217-238, 1980.

Kalnay, E., et al., The NCAR/NCEP 40-year reanalysis project, Bull. Am. Meteorol. Soc., 77, 437-471, 1996.

Keckhut, P., A. Hauchecorne and M.-L. Chanin, A critical review of the data base acquired for the long term surveillance of the middle atmosphere by the French Rayleigh lidar, J. Atmos. Ocean. Technol., 10, 850-867, 1995.

Knittel, J., Ein Beitrag zur Klimatologie der Stratosphaere der Suedhalbkugel, Meteorol. Abh. Met. Inst., Berlin, A2, No. 1, 1974.

Labitzke, K., and collaborators, The Berlin Stratospheric Data Series. CD-rom from Meteorological Institute, Free University of Berlin, 2002.

Lorenc, et al., The Met Office global 3-dimensional variational data assimilation scheme, Q.J.Roy. Meteorol. Soc., 126, 2992-3012, 2000.

Manney, G. L. et al., Comparison of UK meteorological office and US NMC stratospheric analyses during northern and southern winter, J. Geophys. Res., 101, 10,311-10,334, 1996.

Nash, J. and G. F. Forrester, Long-term monitoring of stratospheric temperature trends using radiance measurements obtained by the TIROS-N series of NOAA spacecraft, Adv. Space Res., 6, 37-44, 1986.

Naujokat, B., An update of the observed quasi-biennial oscillation of the stratospheric winds over the tropics, J. Atmos. Sci., 43, 1873-1877, 1986.

Newman, P. A. and E. R. Nash, Quantifying the wave driving of the stratosphere, J. Geophys. Res., 105, 12,485-12,497, 2000.

Oort, A. H., Global atmospheric circulation statistics, 1958-1983, NOAA Professional Paper 14, 1983.

Pawson, S., and co-authors, Climatology of the Northern Hemisphere stratosphere derived from Berlin analyses. Part I. Monthly means, Met. Abh. FU-Berlin, Neue Folge Serie A, Band 7, Heft 3, 1993.

Pawson, S., and co-authors, The GCM-reality intercomparison project for SPARC (GRIPS): Scientific issues and initial results. Bull. Am. Meteorol. Soc., 81, 781-796, 2000.

Pawson, S. and M. Fiorino, A comparison of reanalyses in the tropical stratosphere. Part 1: Thermal structure and the annual cycle, Climate Dyn., 14, 631-644, 1998a.

Pawson, S. and M. Fiorino, A comparison of reanalyses in the tropical stratosphere. Part 2. The quasi-biennial oscillation, Climate Dyn., 14, 645-658, 1998b.

Pawson, S., and B. Naujokat, The cold winters of the middle 1990's in the northern lower stratosphere, J. Geophys. Res., 104, 14,209-14,222, 1999.

Ramaswamy, V., M. L. Chanin, J. Angell, J. Barnett, D. Gaffen, M. Gelman, P. Keckhut, Y. Koshelkov, K. Labitzke, R. Lin, A. O'Neill, J. Nash, W. Randel, R. Rood, K. Shine, M. Shiotani and R. Swinbank, Stratospheric temperature trends: observations and model simulations, Rev. Geophys., 39, 71-122, 2001.

Randel, W. J., The evaluation of winds from geopotential height data in the stratosphere, J. Atmos. Sci., 44, 3097-3120, 1987.

Randel, W. J., Global Atmospheric Circulation Statistics, 1000-1 mb, NCAR Technical Note, NCAR/TN-366 STR, 256 pp., 1992.

Randel, W. J. and F. Wu, Cooling of the Arctic and Antarctic polar stratosplheres due to ozone depletion, J. Climate, 12, 1467-1479, 1999.

Remsberg, E. E., et al., The validation of HALOE temperature profiles in the mesosphere using Rayleigh backscatter lidar and inflatable falling sphere measurements, J. Geophys. Res., submitted, 2002.

Russell, J. M., et al., The Halogen Occulation Experiment, J. Geophys. Res., 98, 10,777-10,979, 1993.

Scaife, A. A., J. Austin, N. Butchart, S. Pawson, M. Keil, J. Nash and I. N. James, Seasonal and interannual variability of the stratosphere diagnosed from UKMO TOVS analyses, Quart. J. R. Meteorol. Soc., 126, 2585-2604, 2000.

Schmidlin, F. J, Rocket techniques used to measure the neutral atmosphere, Middle Atmosphere Program Handbook for MAP Volume 19, edited by Richard A. Goldberg, pp. 1-28 and references therein, March 1986.

Smith, W. L., H. M. Woolf, C. M. Haydex, D. Q. Wark and L. W. McMillin, The TIROS-N operational vertical sounder, Bull. Am. Meteorol. Soc., 60, 1177-1187, 1979.

Stratospheric Processes and Their Role in Climate (SPARC), 2002: SPARC Intercomparison of Middle Atmosphere Climatologies. SPARC Report No. 3, 96 pp., edited by W. Randel, M.-L. Chanin and C. Michant.

Swinbank, R. and A. O'Neill, A stratosphere-troposphere data assimilation system, Monthly Weather Review, 122, 686-702, 1994.

Swinbank, R. and D. A. Ortland, Compilation of wind data for the UARS reference atmosphere project. J. Geophys. Res., submitted 2002.

World Meteorological Organization (WMO), Scientific assessment of ozone depletion: 1998. WMO Report No. 44, Geneva, 1999.

Wu, D. L., W. G. Read, Z. Shippony, T. Leblanc, T. J. Duck, D. A. Ortland, R. J. Sica, P. S. Argall, J. Oberheide, A. Hauchecorne, P. Keckhut, C. She and D. A. Krueger, Mesospheric temperatures from UARS MLS: Retrieval and validation, J. Atmos. Solar-Terr. Phys., submitted 2002.

Figure Captions

Figure 1. Climatological zonal mean zonal winds (top) and temperatures (bottom) for January (left) and July (right). Zonal winds are from the URAP data set (contour interval 5 m/s, with zero contours omitted). Temperatures are from UKMO analyses (1000-1.5 hPa), and a combination of HALOE plus MLS data above 1.5 hPa (see SPARC, 2002). The heavy dashed lines denote the tropopause (taken from NCEP reanalyses) and stratopause (defined by the local temperature maximum near 50 km).

Figure 2. (a) The availability of rocketsonde wind and temperature measurements at 1 hPa as a function of latitude during 1970-1989. Each line represents data from a single station, which are subsequently sampled in latitude bins centered at 10°S, 10°N, 30°N, 60°N and 80°N. (b) The number and latitude distribution of lidar temperature measurements during the 1990's, which contribute to the lidar climatology.

Figure 3. (a) Latitudinal distribution of 100 hPa zonal mean temperature from different analyses for January, together with (b) the distribution of differences between each analysis and UKMO (i.e., NCEP-UKMO, etc.).

Figure 4. Left panels show seasonal variation of 50 hPa zonal mean temperature at 80°N (top) and 80°S (bottom); note the respective time axes have been shifted by 6 months so that winter is in the middle of each plot. Right panels show the corresponding differences from UKMO analyses (i.e., CIRA86-UKMO, etc.).

Figure 5. Comparison of January average rocketsonde temperature statistics at 30°N with zonal mean analyses. Line types identify the same data sets as in Figure 6, and circles show mean rocketsonde values.

Figure 6. Comparison of the seasonal variation of rocketsonde temperatures near 30°N with zonal mean analyses, for pressure levels 0.1 hPa (top) and 1 hPa (bottom). Circles denote the rocketsonde means, and error bars the plus/minus one standard error.

Figure 7. Comparison of the seasonal variation of lidar temperatures near 40°N with zonal mean analyses. Circles denote the lidar means, and error bars the plus/minus one standard error.

Figure 8. Comparison of the vertical profile of temperature near 80°N between lidar measurements and zonal mean analyses, for statistics during December-February.

Figure 9. Comparison of the seasonal variation in equatorial zonal mean temperature from available analyses at 50 hPa (top) and 100 hPa (bottom). The circles show a climatology derived from radiosonde measurements at eight near-equatorial stations (over 5°N-5°S), and the error bars denote the plus/minus standard error of the mean.

Figure 10. (a) Latitudinal structure of the amplitude of the temperature SAO at 2 hPa derived from each data set. The dots show the corresponding values derived from rocketsonde data near 8°S and 8°N. (b) and (c) Show the vertical amplitude and phase structure of the SAO at the equator. Phase refers to month of the first maximum during the calendar year. The open circles show the mesospheric results derived from SME satellite data, taken from Garcia and Clancy (1990).

Figure 11. Meridional cross sections of differences in January zonal mean zonal wind from UKMO analyses, showing results for CPC (top), ERA40 (middle), and CIRA86 (bottom). Contour intervals are ± 2, 4, 6 ... m/s.

Figure 12. Comparison of the seasonal variation of zonal winds measured by rocketsondes with zonal mean analyses at 10°S (left) and 30°N (right), for statistics at 0.1 hPa (top) and 5 hPa (bottom).

Figure 13. (a) Latitudinal structure of the zonal wind SAO at 1 hPa derived from each data set. Dots show rocketsonde results at 8°N and 8°S. (b) and (c) show the vertical amplitude and phase of the zonal wind SAO at the equator. The phase refers to the time of the first maximum during the calendar year.

Figure 14. Time series of interannual anomalies in equatorial zonal mean winds during 1988-1997 at 10 and 30 hPa from various analyses and from Singapore (1°N) radiosonde measurements. Each data set has been deseasonalized with respect to the 1992-1997 means.

Figure 15. (a) Latitudinal structure of the equivalent QBO amplitude in zonal wind at 30 hPa, defined as $\sqrt{2}$ times the rms anomaly values during 1992-1997 (see text). (b) Shows the vertical structure of QBO amplitude at the equator. For comparison, results of Dunkerton and Delisi (1985) are shown, together with estimates from Singapore radiosondes, and results derived from rocketsondes for 1970-1989.

Figure 16. Seasonal variation of zonal mean eddy heat flux $\left(\overline{v'T'}\right)$ at 100 hPa in the NH (40-70°N, left) and in the SH (40-70°S, right), derived from CPC, NCEP,

ERA40 and UKMO analyses over 1992-1997. The NH minimum in February is not a climatological feature, but results from this small time sample.

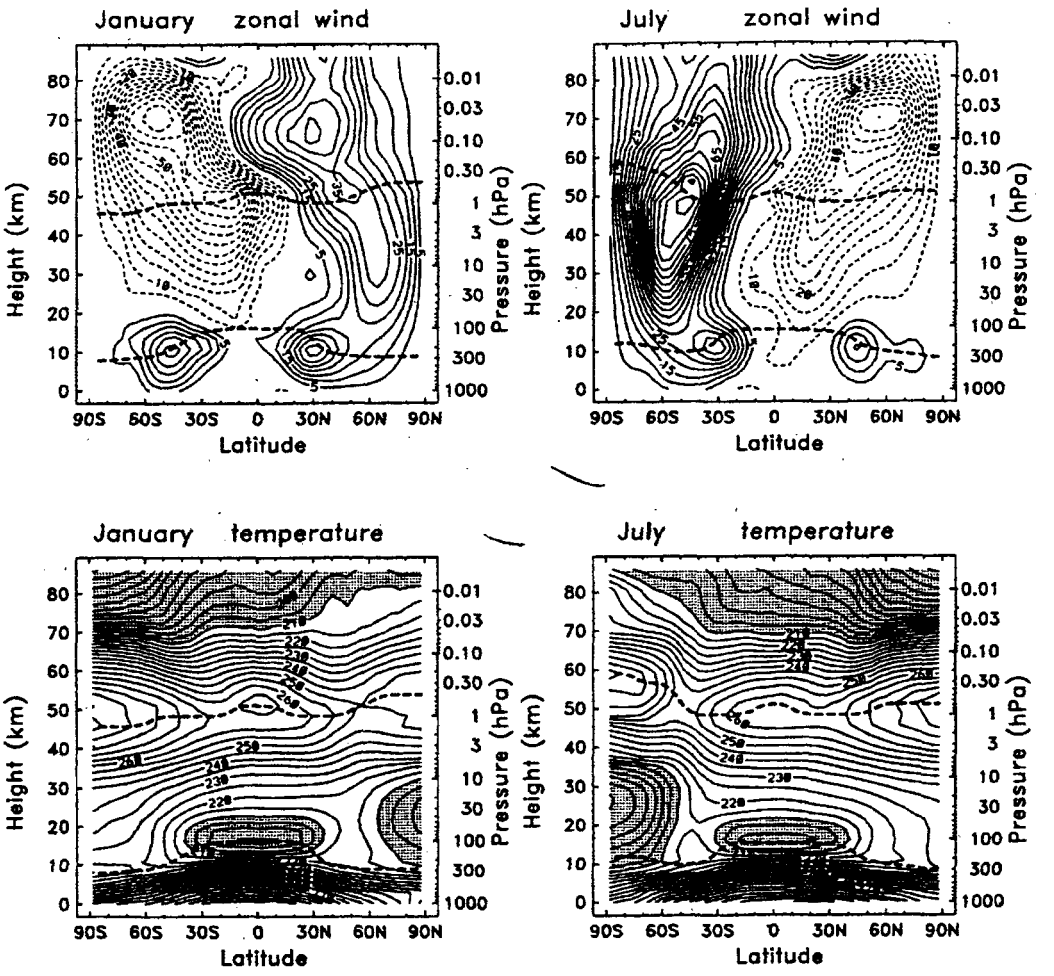

Figure 1. Climatological zonal mean zonal winds (top) and temperatures (bottom) for January (left) and July (right). Zonal winds are from the URAP data set (contour interval 5 m/s, with zero contours omitted). Temperatures are from UKMO analyses (1000-1.5 hPa), and a combination of HALOE plus MLS data above 1.5 hPa (see SPARC, 2002). The heavy dashed lines denote the tropopause (taken from NCEP reanalyses) and stratopause (defined by the local temperature maximum near 50 km).

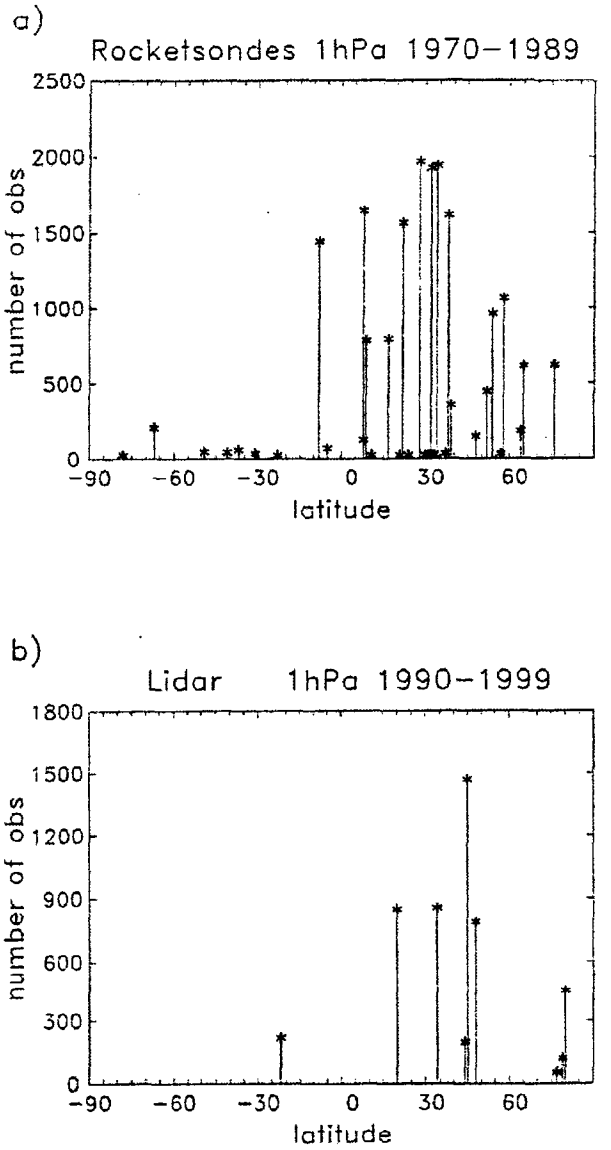

Figure 2. (a) The availability of rocketsonde wind and temperature measurements at 1 hPa as a function of latitude during 1970-1989. Each line represents data from a single station, which are subsequently sampled in latitude bins centered at 10°S, 10°N, 30°N, 60°N and 80°N. (b) The number and latitude distribution of lidar temperature measurements during the 1990's, which contribute to the lidar climatology.

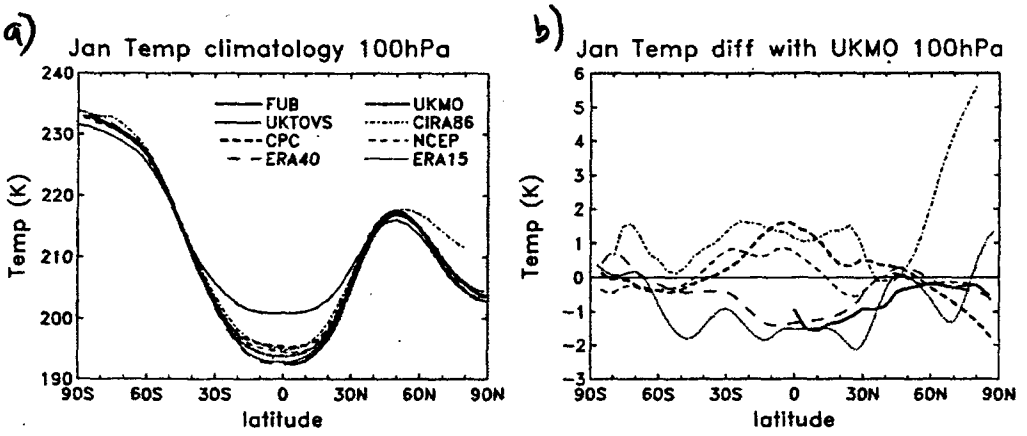

Figure 3. (a) Latitudinal distribution of 100 hPa zonal mean temperature from different analyses for January, together with (b) the distribution of differences between each analysis and UKMO (i.e., NCEP-UKMO, etc.).

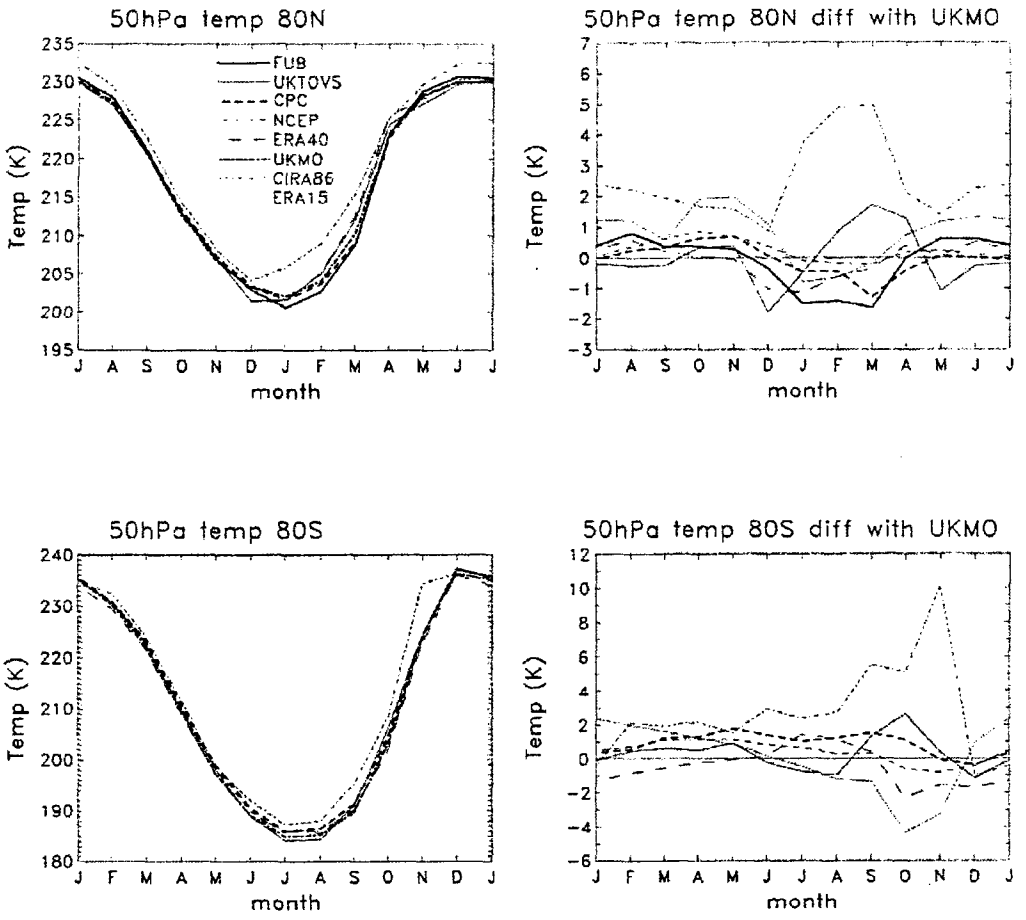

Figure 4. Left panels show seasonal variation of 50 hPa zonal mean temperature at 80°N (top) and 80°S (bottom): note the respective time axes have been shifted by 6 months so that winter is in the middle of each plot. Right panels show the corresponding differences from UKMO analyses (i.e., CIRA86-UKMO, etc.).

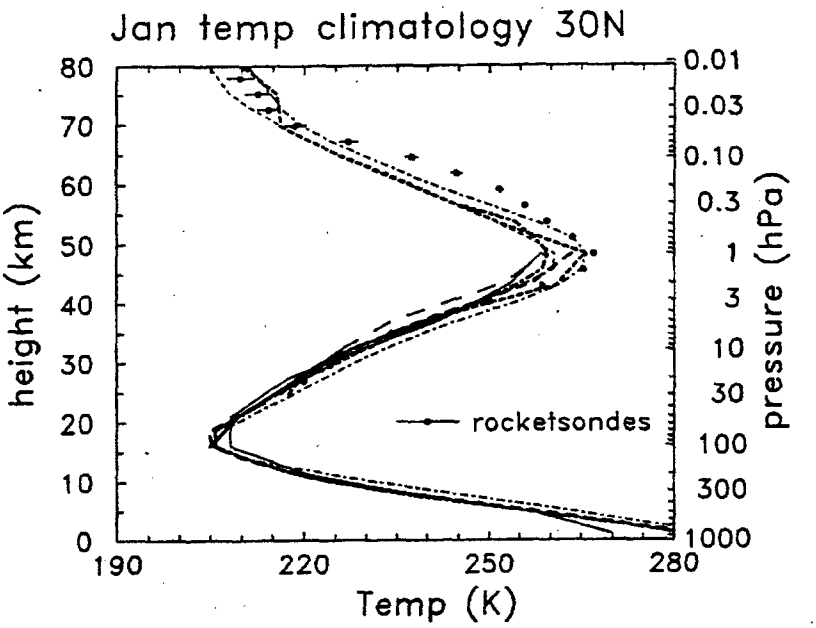

Figure 5. Comparison of January average rocketsonde temperature statistics at 30°N with zonal mean analyses. Line types identify the same data sets as in Figure 6, and circles show mean rocketsonde values.

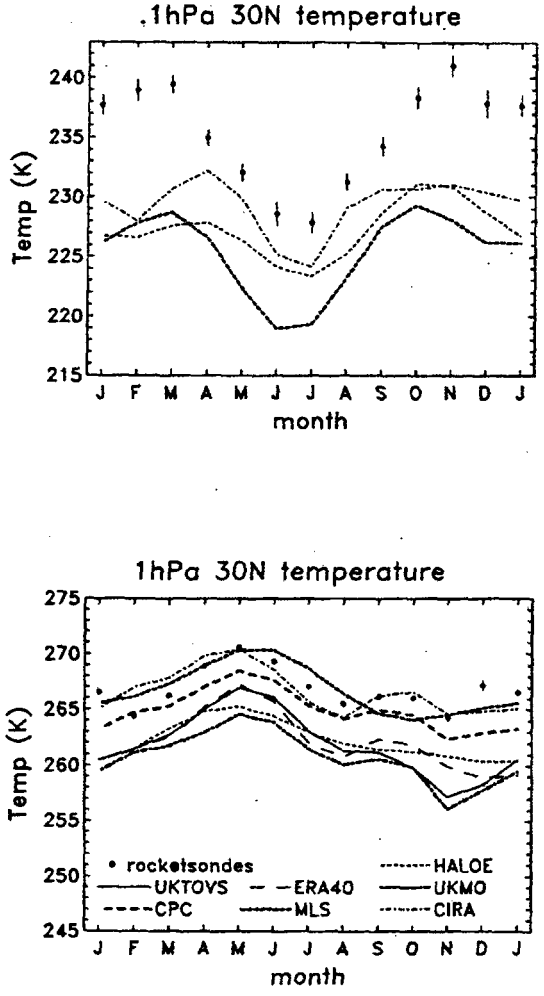

Figure 6. Comparison of the seasonal variation of rocketsonde temperatures near 30°N with zonal mean analyses, for pressure levels 0.1 hPa (top) and 1 hPa (bottom). Circles denote the rocketsonde means, and error bars the plus/minus one standard error.

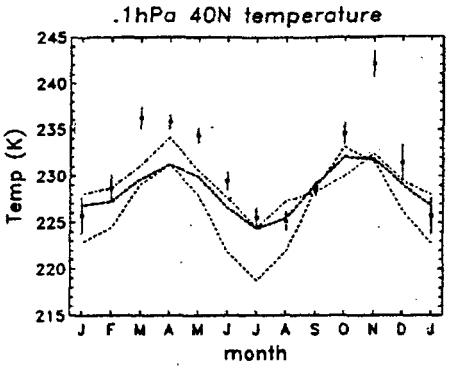

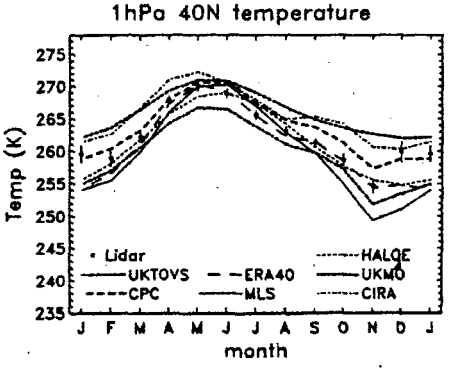

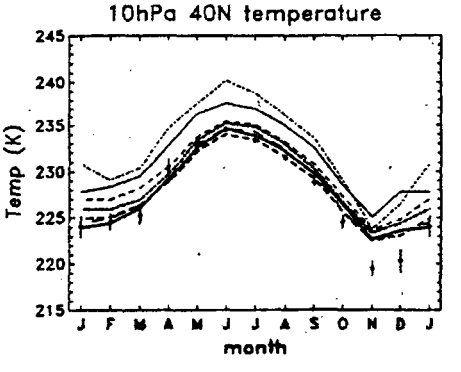

Figure 7. Comparison of the seasonal variation of lidar temperatures near 40°N with zonal mean analyses. Circles denote the lidar means, and error bars the plus/minus one standard error.

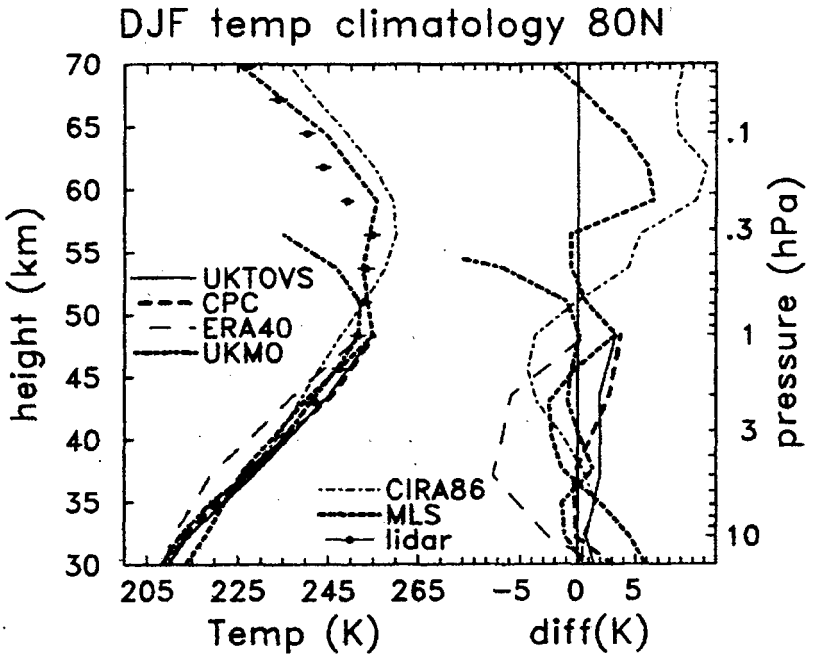

Figure 8. Comparison of the vertical profile of temperature near ~~80°N between lidar~~ measurements and zonal mean analyses, for statistics during December-February.

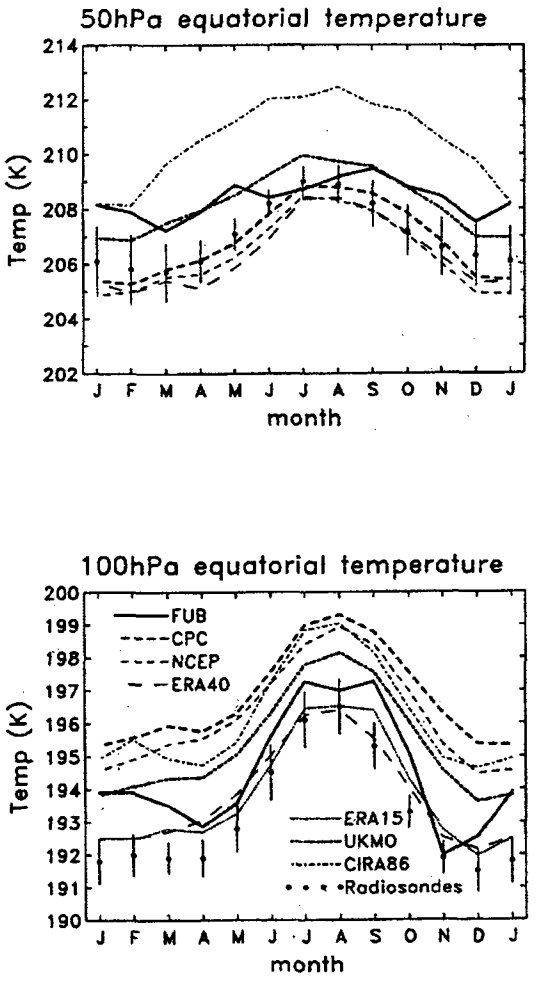

Figure 9. Comparison of the seasonal variation in equatorial zonal mean temperature from available analyses at 50 hPa (top) and 100 hPa (bottom). The circles show a climatology derived from radiosonde measurements at eight near-equatorial stations (over 5°N-5°S), and the error bars denote the plus/minus standard error of the mean.

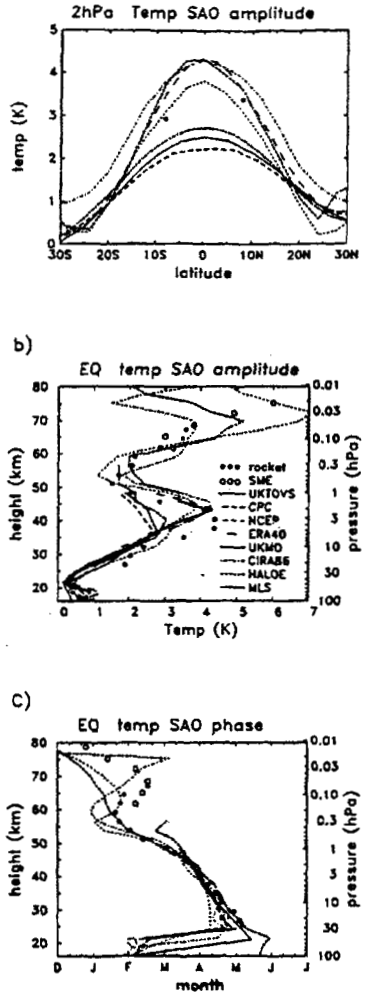

Figure 10. (a) Latitudinal structure of the amplitude of the temperature SAO at 2 hPa derived from each data set. The dots show the corresponding values derived from rocketsonde data near 8°S and 8°N. (b) and (c) Show the vertical amplitude and phase structure of the SAO at the equator. Phase refers to month of the first maximum during the calendar year. The open circles show the mesospheric results derived from SME satellite data, taken from Garcia and Clancy (1990).

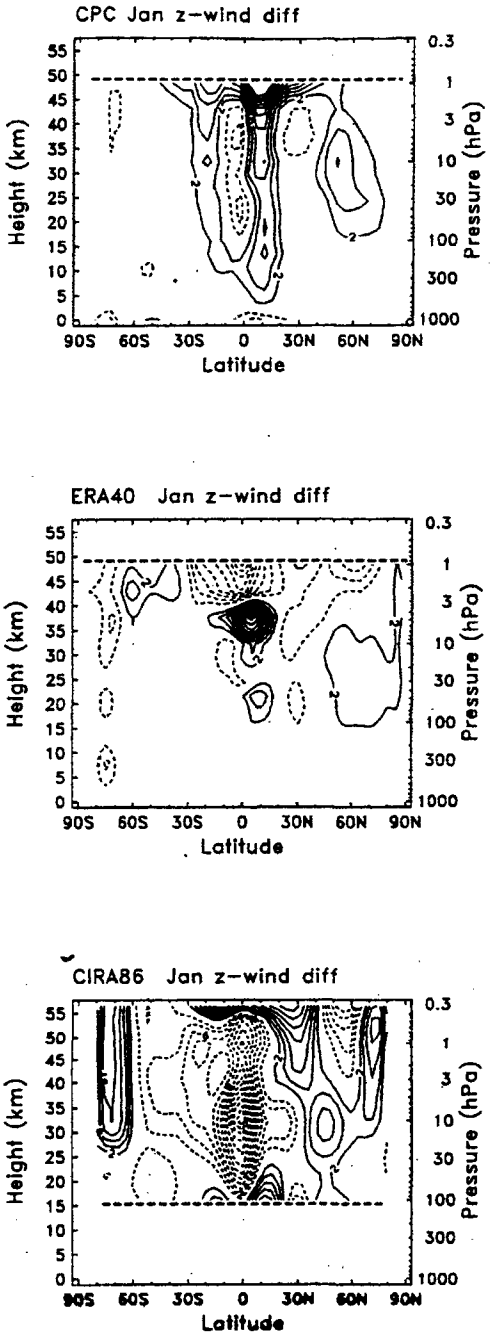

Figure 11. Meridional cross sections of differences in January zonal mean zonal wind from UKMO analyses, showing results for CPC (top), ERA40 (middle), and CIRA86 (bottom). .Contour intervals are ± 2, 4, 6 ... m/s.

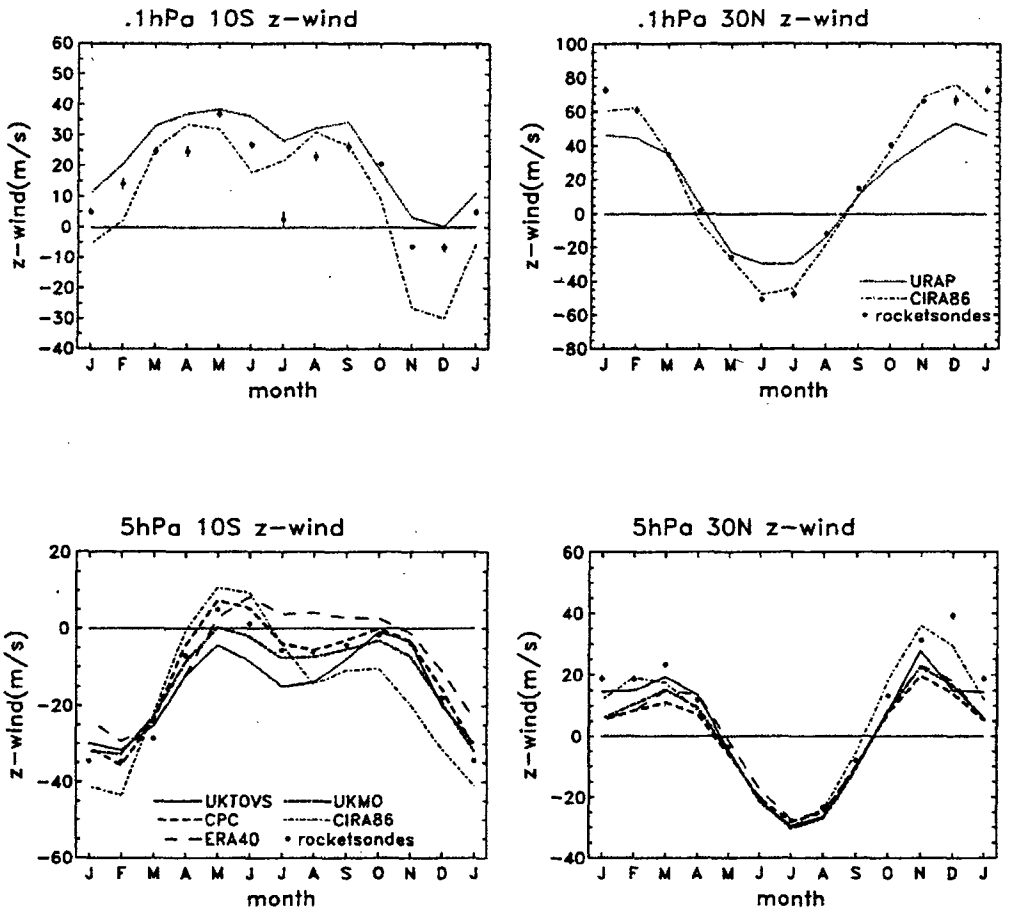

Figure 12. Comparison of the seasonal variation of zonal winds measured by rocketsondes with zonal mean analyses at 10°S (left) and 30°N (right), for statistics at 0.1 hPa (top) and 5 hPa (bottom).

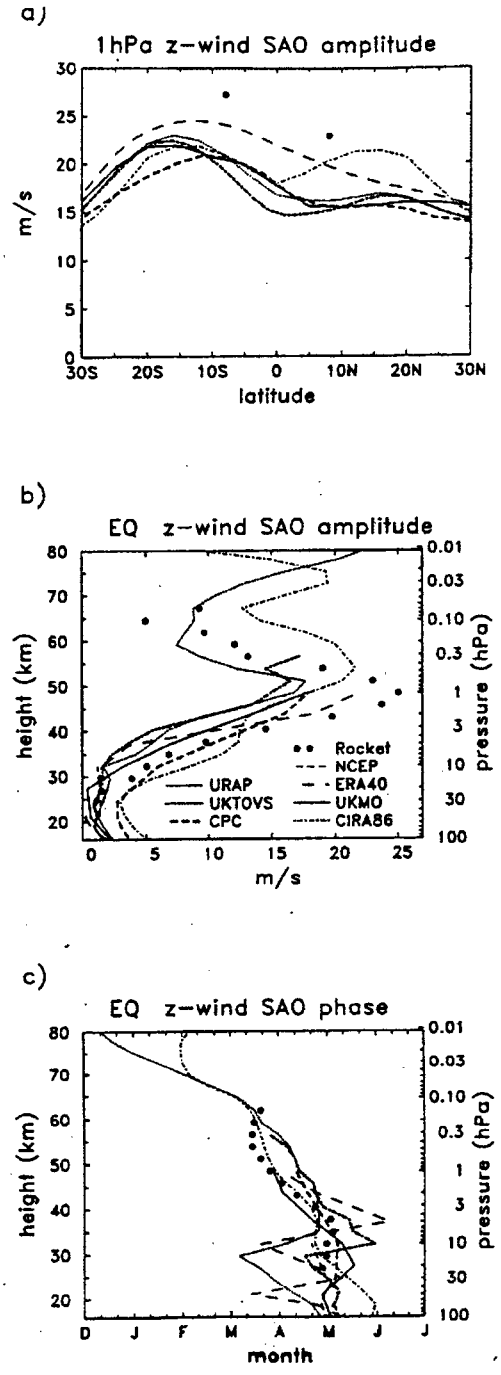

Figure 13. (a) Latitudinal structure of the zonal wind SAO at 1 hPa derived from each data set. Dots show rocketsonde results at 8°N and 8°S. (b) and (c) show the vertical amplitude and phase of the zonal wind SAO at the equator. The phase refers to the time of the first maximum during the calendar year.

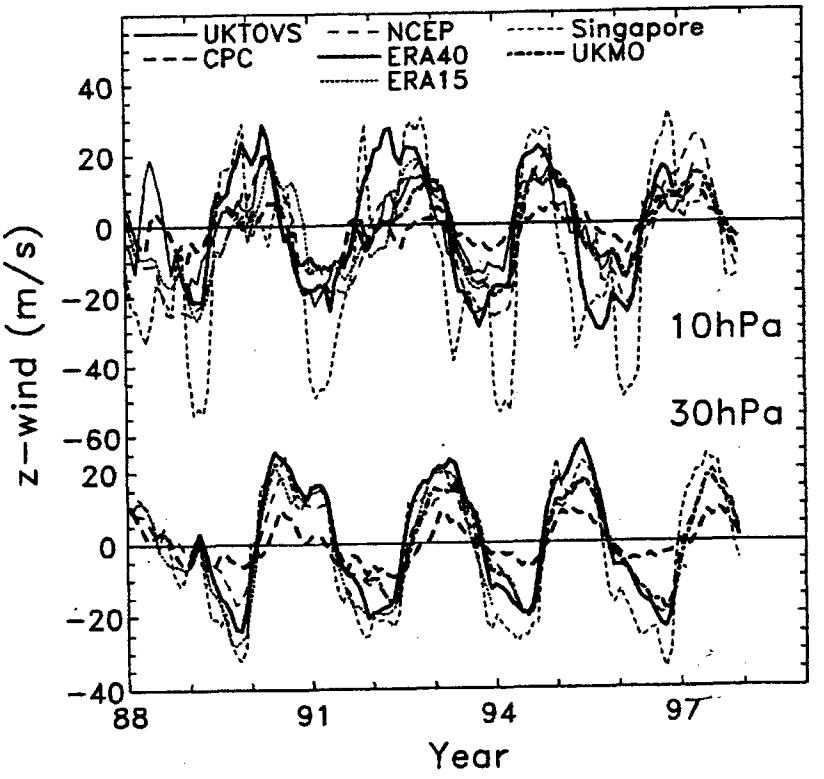

Figure 14. Time series of interannual anomalies in equatorial zonal mean winds during 1988-1997 at 10 and 30 hPa from various analyses and from Singapore (1°N) radiosonde measurements. Each data set has been deseasonalized with respect to the 1992-1997 means.

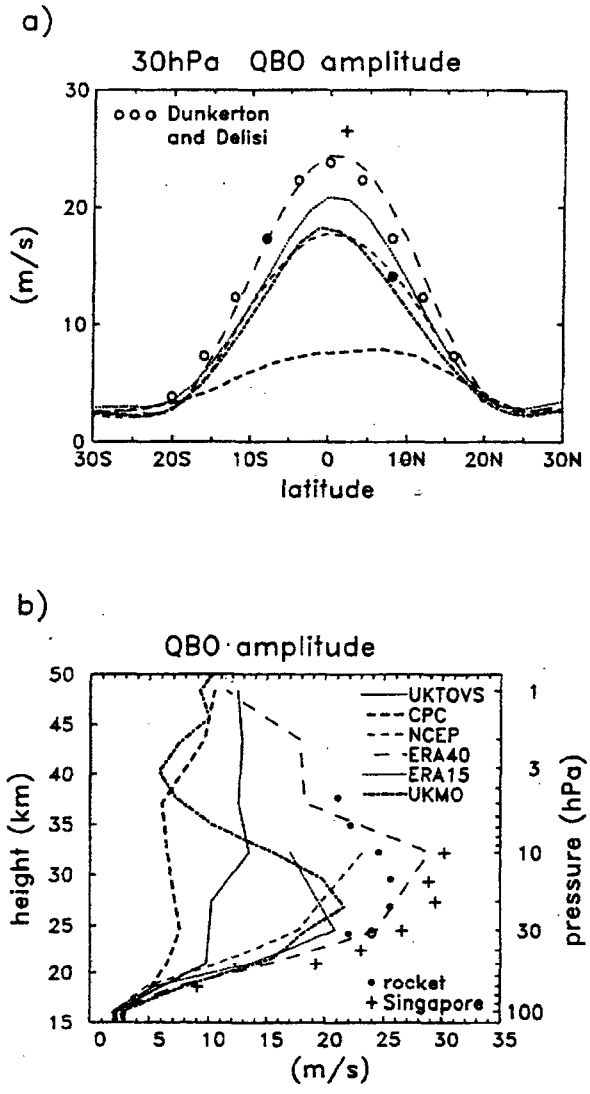

Figure 15. (a) Latitudinal structure of the equivalent QBO amplitude in zonal wind at 30 hPa, defined as $\sqrt{2}$ times the rms anomaly values during 1992-1997 (see text). (b) Shows the vertical structure of QBO amplitude at the equator. For comparison, results of Dunkerton and Delisi (1985) are shown, together with estimates from Singapore radiosondes, and results derived from rocketsondes for 1970-1989.

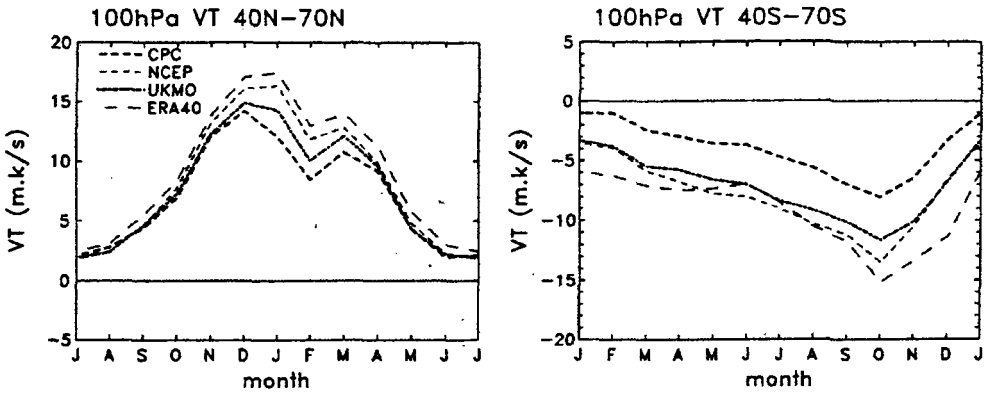

Figure 16. Seasonal variation of zonal mean eddy heat flux $\left(\overline{v'T'}\right)$ at 100 hPa in the NH (40-70°N, left) and in the SH (40-70°S, right), derived from CPC, NCEP, ERA40 and UKMO analyses over 1992-1997. The NH minimum in February is not a climatological feature, but results from this small time sample.